

Two-Dimensional Gradient-Index Metamaterial with Sawtooth Profile

Zoran Jakšić¹, Milija Sarajlić¹, Žarko Lazić¹, Mariana Dalarsson²,
Danijela Randjelović¹, Katarina Radulović¹, Dragan Tanasković¹

Abstract – We investigate theoretically and experimentally a binary metal-dielectric metamaterial with a sawtooth profile. The structure consists of a two-dimensional array of pillars with submicrometer diameters. The pillar diameters linearly vary along one axis and are constant along the other. This furnishes a serrated spatial profile of effective refractive index along a single axis. We first present a set of analytical solutions defining the electromagnetic fields in such a structure. Further we give the results of our experimental fabrication of gradient metamaterial with a sawtooth spatial profile. The basic material for pillars was photoresist. Their geometry was defined using direct laser writing. Resist was overexposed in controlled manner in order to obtain pillars with diameters below the nominal resolution of the laser writer. The microfabricated pillars were coated by a sputter-deposited aluminum film. For characterization we utilized optical and atomic force microscopy and angle-dependent Fourier Transform infrared spectroscopy. We envision the applicability of our graded metasurfaces in transformation optics.

Keywords – Metamaterials, Metal-Dielectrics, Frequency-Selective Surfaces, Microfabrication.

I. INTRODUCTION

Metamaterials are artificial structures with properties not readily found in nature [1]. Probably the best known electromagnetic metamaterials are those with negative values

of effective refractive index. More generally, an electromagnetic metamaterial may be defined as a structure enabling a complete control over frequency dispersion [2]. Extreme values of group velocity are attainable, including superluminal ones ("fast light"), very low and near-zero values ("slow light" or even "stopped light") and values below zero ("left-handed light") [3]. Correspondingly, the effective refractive index can be tailored to reach extreme values, including high, near-zero and negative values. Typical practical implementations of metamaterials include ordered 1D, 2D or 3D arrays of basic patterns (artificial "atoms" or "molecules" of metamaterial) with dimensions much smaller than the operating wavelength [4]. The subwavelength nature of these patterns allows one to apply the effective medium approach [5] and calculate electromagnetic parameters in a fashion similar to that applied to natural atoms/molecules when determining their properties.

The next step of designer freedom is offered by a possibility to tailor the spatial dispersion of metamaterial properties, i.e. to utilize metamaterials with spatial gradient of refractive index [6-8]. The gradient index (GRIN) optics [9-11] itself is very old and James Clerk Maxwell himself described the first GRIN optical element, the fish-eye lens. With the ability to tailor frequency dispersion offered by metamaterials the gradient index optics has reached a new peak. This synergy resulted in the introduction and development of the transformation optics [12-14] which ensures a full control over flow of electromagnetic energy. This new field of electromagnetics utilizes conformal transformations to make possible new structures and devices with properties previously thought impossible. One of the more widely known such applications are the so-called invisibility cloaks [15], experimentally fabricated for the near-optical range as carpet cloaks [16]. Many other applications of transformation optics have been described, including different kinds of metamaterial lenses like Lüneburg [17] and Maxwell's fish-eye [18], but also different optical elements like super-absorbers [19], super-concentrators [20], hyperlenses for far-field subwavelength imaging [21-22] and many more. It may be safely said that graded refractive index metamaterials not only offer a new degree of freedom for an array of practical applications, but enable opening a completely new paradigm in electromagnetics.

The main problem with the fabrication of metamaterial structures for the optical range, including visible and near infrared, is that the building blocks must be much smaller than the operating wavelength. This is valid both for isotropic and for graded optical metamaterials. Expensive and complex

¹Zoran Jakšić is with the Center of Microelectronic Technologies, ICTM, University of Belgrade, Njegoševa 12, 11000 Belgrade, Serbia, E-mail: jaksa@nanosys.ihtm.bg.ac.rs.

¹Milija Sarajlić is with the Center of Microelectronic Technologies, ICTM, University of Belgrade, Njegoševa 12, 11000 Belgrade, Serbia, E-mail: milijas@nanosys.ihtm.bg.ac.rs.

¹Žarko Lazić is with the Center of Microelectronic Technologies, ICTM, University of Belgrade, Njegoševa 12, 11000 Belgrade, Serbia, E-mail: zlazic@nanosys.ihtm.bg.ac.rs.

²Mariana Dalarsson is with the Division of Electromagnetic Engineering, School of El. Eng., Royal Institute of Technology, SE-100 44 Stockholm, Sweden, E-mail: mariana.dalarsson@ee.kth.se.

¹Danijela Randjelović is with the Center of Microelectronic Technologies, ICTM, University of Belgrade, Njegoševa 12, 11000 Belgrade, Serbia, E-mail: danijela@nanosys.ihtm.bg.ac.rs.

¹Katarina Radulović is with the Center of Microelectronic Technologies, ICTM, University of Belgrade, Njegoševa 12, 11000 Belgrade, Serbia, E-mail: kacar@nanosys.ihtm.bg.ac.rs.

¹Dragan Tanasković is with the Center of Microelectronic Technologies, ICTM, University of Belgrade, Njegoševa 12, 11000 Belgrade, Serbia, E-mail: dragant@nanosys.ihtm.bg.ac.rs.

nanofabrication procedures are necessary even for 2D arrays, while 3D structures are much more complex to produce. The degree of complexity increases with decreasing wavelength and is probably the highest for the structures belonging to nanoplasmonics, i.e. those metamaterials whose function relies on the propagation of evanescent waves between a positive and negative dielectric permittivity material (plasmonic crystals) [23].

In this paper we consider a possibility to use relatively inexpensive microlithography for the fabrication of graded arrays of nanopillars and to utilize overexposure to enter the sub-micrometer range with the characteristic dimensions. We use inhomogeneous exposure to obtain uniformly varying pillar diameter along one dimension.

II. ANALYTICAL

The spatial distribution of electric and magnetic field can be determined utilizing an exact analytical approach [24, 25].

The starting point from our *ab initio* analysis are Maxwell's equations. We assume that our metamaterial is a binary composite medium with periodically alternating materials which are described by their relative dielectric permittivity and relative magnetic permeability. Both permittivity and permeability can have real and imaginary parts, i.e. we consider a lossy case where absorption is not neglected. At least one of these materials can be described by Drude or Lorentz dispersion, i.e. its permittivity is lower than zero in a certain wavelength range. In a general case this material will have negative refractive index, while the alternating one will have a positive value.

We assume that the effective medium approximation is applicable to our metamaterial, i.e. that its constituent parts are much smaller than the operating wavelength. Thus the electromagnetic properties can be described by the effective relative dielectric permittivity and the effective relative magnetic permeability. For most metamaterials, the effective medium assumption is valid, because their constituent elements size is on the subwavelength level.

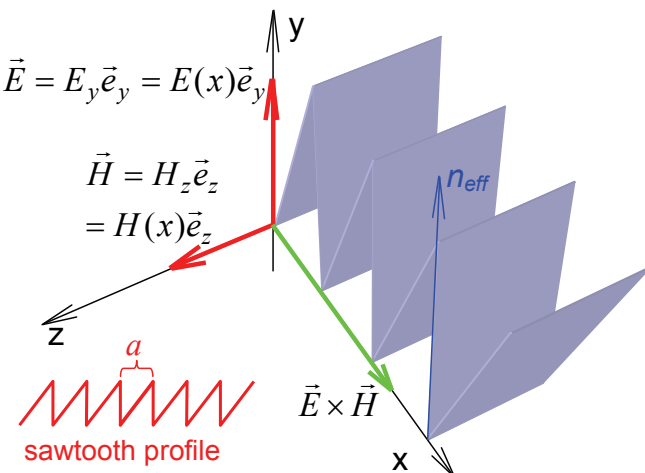


Fig. 1. Propagation of an EM wave through a graded index structure with a sawtooth profile

Figure 1 represents propagation of an electromagnetic wave along the x-axis of a gradient index structure with a sawtooth profile. The electric field is directed along the y-axis, $\vec{E}(\vec{r}) = E_y \vec{e}_y = E(x) \vec{e}_y$, and the magnetic field is directed along the z-axis, $\vec{H}(\vec{r}) = H_z \vec{e}_z = H(x) \vec{e}_z$. Thus the Pointing vector and the propagation direction of the wave are oriented along the x-axis.

Since the electric and magnetic field depend only on one coordinate, the source-free Maxwell equations are

$$\begin{aligned}\frac{dE}{dx} &= -i\omega\mu H, \\ \frac{dH}{dx} &= -i\omega\epsilon E,\end{aligned}\quad (1)$$

where the dielectric permittivity is $\epsilon = \epsilon(\omega, x)$ and the magnetic permeability $\mu = \mu(\omega, x)$. Both of these are frequency- and space-dependent.

The Helmholtz' equations are obtained by eliminating either the magnetic field

$$\frac{d^2E}{dx^2} - \frac{1}{\mu} \frac{d\mu}{dx} \frac{dE}{dx} + \omega^2 \mu \epsilon E(x) = 0 \quad (2)$$

or the electric field

$$\frac{d^2H}{dx^2} - \frac{1}{\epsilon} \frac{d\epsilon}{dx} \frac{dH}{dx} + \omega^2 \mu \epsilon H(x) = 0 \quad (3)$$

Let us now consider the effective permittivity and permeability of the metamaterial composite. We assume that the spatial dependence of the real parts of the effective permittivity and permeability is described by an arbitrary periodic function $f(x)$. Thus the effective parameters can be represented as

$$\begin{aligned}\epsilon(\omega, x) &= -\epsilon_0 [\epsilon_r(\omega)f(x) - i\epsilon_i(\omega)], \\ \mu(\omega, x) &= -\mu_0 [\mu_r(\omega)f(x) - i\mu_i(\omega)].\end{aligned}\quad (3)$$

where $-1 \leq f(x) \leq +1$.

We assume that our composite material is passive, i.e. there is no amplification of radiation in any of its parts. In other words, no lasing medium and external pumping are used within it and absorption losses in both constituents of the binary composite are larger than zero, i.e.

$$\begin{aligned}\epsilon_f(\omega) &> 0, \\ \mu_f(\omega) &> 0.\end{aligned}\quad (4)\quad (5)$$

Here we further assume that there is no reflection on the graded interfaces between the two materials comprising the binary composite. In other words, we require a constant wave impedance throughout the structure:

$$Z = Z_0 Z(\omega) = \sqrt{\mu_0 \mu_R(\omega) / \epsilon_0 \epsilon_R(\omega)} \quad (6)$$

In order for this condition to be fulfilled, the real and imaginary parts of the effective permittivity and permeability must satisfy the condition

$$\frac{\mu_I(\omega)}{\mu_R(\omega)} = \frac{\varepsilon_I(\omega)}{\varepsilon_R(\omega)} = \beta(\omega) . \quad (7)$$

This is the basic limitation of our analytical model regarding the properties of the material

Thus we have

$$\mu = -\mu_0 \mu_R(\omega) [f(x) + i\beta] , \quad (8)$$

$$\varepsilon = -\varepsilon_0 \varepsilon_R(\omega) [f(x) + i\beta] . \quad (9)$$

The exact analytical solution to (1), (2) has the remarkably simple form

$$\begin{aligned} E(x) &= E(0) \exp(-k\beta x) \exp[-ikF(x)] \\ H(x) &= H(0) \exp(-k\beta x) \exp[-ikF(x)] \\ F(x) &= \int_0^x f(\xi) d\xi \\ k &= \sqrt{-\varepsilon_0 \mu_0 \omega^2 \varepsilon_r(\omega) \mu_r(\omega)} \end{aligned} \quad (10)$$

where $E(0)$ and $H(0)$ are the amplitudes of the electric and magnetic fields at $x = 0$. The solution (6) is completely general within the context of the quoted assumptions.

Now we consider the case of the simple sinusoidal spatial dependence

$$f(x) = \cos\left(\frac{\pi}{a}x\right) , \quad (11)$$

where a is the thickness of a layer pair. The expressions for the electric and magnetic field are then obtained as

$$E(x) = E_0 e^{-k\beta x} \exp\left(-i \frac{ka}{\pi} \sin \frac{\pi x}{a}\right) , \quad (12)$$

$$H(x) = H_0 e^{-k\beta x} \exp\left(-i \frac{ka}{\pi} \sin \frac{\pi x}{a}\right) . \quad (13)$$

According to Maxwell's equations (1), the field amplitudes are related as $E_0 = Z_0 Z(\omega) H_0$.

In an arbitrary case a periodic function $f(x)$ where $-1 \leq f(x) \leq +1$, can be represented by a Fourier series expansion. For instance, if $f(x)$ is an even function with period $2a$, its Fourier expansion is

$$f(x) = \sum_{m=0}^{\infty} \alpha_m \cos\left(\frac{m\pi}{a}x\right) . \quad (14)$$

Thus the electric and magnetic field are

$$E(x) = E_0 e^{-k\beta x} \exp\left(-i \frac{ka}{\pi} \sum_{m=0}^{\infty} \frac{\alpha_m}{m} \sin\left(\frac{m\pi}{a}x\right)\right) , \quad (15)$$

$$H(x) = H_0 e^{-k\beta x} \exp\left(-i \frac{ka}{\pi} \sum_{m=0}^{\infty} \frac{\alpha_m}{m} \sin\left(\frac{m\pi}{a}x\right)\right) , \quad (16)$$

If a single layer within the observed composite is described by positive refractive index, for $x \rightarrow 0$ it is obtained that

$$E(x) = E_0 e^{-k\beta x} \exp(-ikx) , \quad (17)$$

$$H(x) = H_0 e^{-k\beta x} \exp(-ikx) , \quad (18)$$

since it is valid for the Fourier coefficients that

$$\sum_{m=0}^{\infty} \alpha_m = 1 , \quad (19)$$

In the time-domain the fields are

$$E(x) \sim E_0 e^{-k\beta x} \cos(\omega t - kx) , \quad (20)$$

$$H(x) \sim H_0 e^{-k\beta x} \cos(\omega t - kx) , \quad (21)$$

For a single layer with negative refractive index at $x \rightarrow (a/2)_+$ we obtain in equivalent fashion

$$E(x) = E_0 e^{-k\beta x} \exp(+ikx) , \quad (22)$$

$$H(x) = H_0 e^{-k\beta x} \exp(+ikx) , \quad (23)$$

and in the time-domain

$$E(x) \sim E_0 e^{-k\beta x} \cos(\omega t - (-k)x) , \quad (24)$$

$$H(x) \sim H_0 e^{-k\beta x} \cos(\omega t - (-k)x) . \quad (25)$$

From the results (20)-(21), it follows that the asymptotic wavevector in the PIM layers is $\vec{k}_{RHM} = +k\vec{e}_x$, i.e. the wave propagates in the $+x$ -direction. On the other hand the asymptotic wavevector in the NIM layers is $\vec{k}_{LHM} = -k\vec{e}_x$, i.e. the wave propagates in the $-x$ -direction. However, the energy flux (the Poynting vector) is still in the $+x$ -direction in both media.

In this particular case we are interested in calculating a sawtooth dependence, i.e. a periodical function with a linear dependence within a single period.

If we denote the width of the linear transition layer by a , for the case shown in Fig. 1 the form of the function $f(x)$ will be

$$f(x) = \frac{2}{\pi} \sum_{m=1}^{\infty} \frac{(-1)^{m+1}}{m} \sin\left(\frac{m\pi}{a}x\right) , \quad (26)$$

and the solution for the electric field

$$E(x) = E_0 e^{-k\beta x} \exp\left(i \frac{ka}{\pi} \sum_{m=1}^{\infty} \frac{(-1)^{m+1}}{m^2} \cos\left(\frac{m\pi}{a}x\right) - \frac{\pi^2}{12}\right) \quad (27)$$

with an equivalent form for the spatial dependence of the magnetic field.

As an illustration, Fig. 2 shows the variation of the electric field across a sample with a sawtooth periodic dependence.

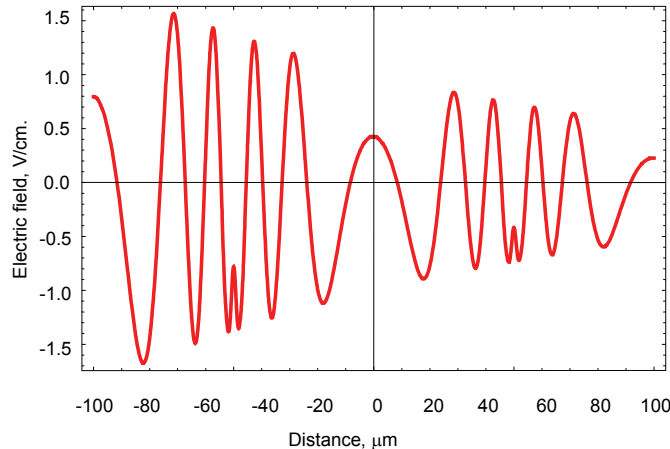


Fig. 2. Analytical results for the real part of electric field $E(x)$ as a function of x , with a width of a spatial period $a = 100 \mu\text{m}$ and a loss factor of $\beta = 10^{-2}$

III. DESIGN OF BINARY METAMATERIAL COMPOSITE

The practical implementation of the graded structure considered in the previous Section is shown in Fig. 3. A square 2D array of subwavelength pillars is formed at a substrate surface. The radii of the pillars linearly increase along the x -axis for a certain spatial period, then return to their original value. This repeats periodically, thus forming a sawtooth-shaped profile of effective refractive index along the x -axis. The radii remain constant along the z -axis.

The gradient of effective refractive index is ensured by utilizing 2D arrays of pillars whose diameters varies linearly along the x -axis and is constant along the z -axis. In this manner a single pillar assumes the role of a meta-“atom” of the structure. Each row of thus designed meta-atoms at a given x -position has different electromagnetic properties since its corresponding filling factor is determined by its diameter. Thus according to the effective medium approximation it will define a certain value of the effective refractive index which will vary along the x -axis in a sawtooth fashion. The presence of metal will mean that the absorption losses (the imaginary part of the index) will not be negligible.

Obviously, the electromagnetic properties of the structure will be strongly anisotropic and dependent on the direction of the electromagnetic field. Within this paper, we will analyze only the waves propagating along the x -axis direction.

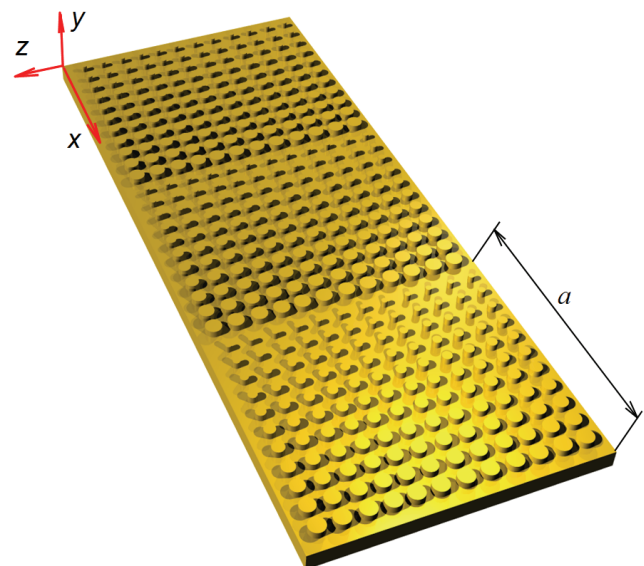


Fig. 3. Implementation of metamaterial with a sawtooth-profile of refractive index utilizing nanopillars with varying diameter

IV. EXPERIMENTAL

The substrate for the fabrication of graded effective index structure was a polished microscopic glass slab 1 mm thick. A layer of positive photoresist AZ 1505 (MicroChemicals, Germany) was spin-coated to the substrate using ST 143 spinner Convac at a speed of 4000 min^{-1} during 30 seconds. Photoresist was dried 15 minutes at 100°C and a $0.5 \mu\text{m}$ thick layer was obtained.

Resist exposition was performed using a LaserWriter LW405. The pattern consisted of parallel strips $2 \mu\text{m}$ wide at a distance of $2 \mu\text{m}$. Another identical pattern was written over the first one, but rotated 90° . In this manner a rectangular net was drawn with non-exposed “islands” between the strips. A total area of $5 \text{ mm} \times 5 \text{ mm}$ was exposed.

In order to obtain smaller “islands”, the wafer was overexposed in a controlled manner and wider strips were obtained than without overexposure. In this manner the equipment intended for micrometer-resolutions has been utilized to define submicrometer features.

Another particularity of the procedure was that inhomogeneous illumination was used. The strips were drawn in $100 \mu\text{m}$ wide swaths (25 strips each), containing wide stripes within which illumination linearly decreased with coordinate. Higher illumination resulted in narrower “islands” and vice versa.

After photoresist was developed in developer AZ 726 MIF Electronic Materials and the wafer was baked at 100°C for 30 minutes, the unexposed islands remained as roughly circular pillars approximately 142 nm high (standard deviation 8.15 nm), with diameters linearly varying across a single stripe from 700 nm to 1200 nm .

The final step was the deposition of aluminum over the pillar array utilizing radiofrequency sputtering at Perkin Elmer equipment. Starting vacuum was $4 \cdot 10^{-4} \text{ Pa}$, argon partial pressure 2 Pa , at 750 W RF power and a target voltage 1000 V

during 2 min 30 s. The thickness of the Al layer of 68 nm was measured utilizing Talystep profilometer.

Characterization of the obtained profile was done at an NTEGRA Prima Atomic Force Microscope NT-MDT utilizing the contactless method. An obtained micrograph is shown in Fig. 4. The spatially varying radius of the pillars is readily observed. The exact dimensions of the pillars were also determined during the AFM measurement.

The next step were reflection measurement in the near infrared (1.0–2.5 μm) utilizing a FTIR spectrometer (Nicolet 6700, Thermo Scientific.) Spectra were measured under different incident angles – 40°, 50° and 60°. The obtained spectra are shown in Figs. 5 and 6.

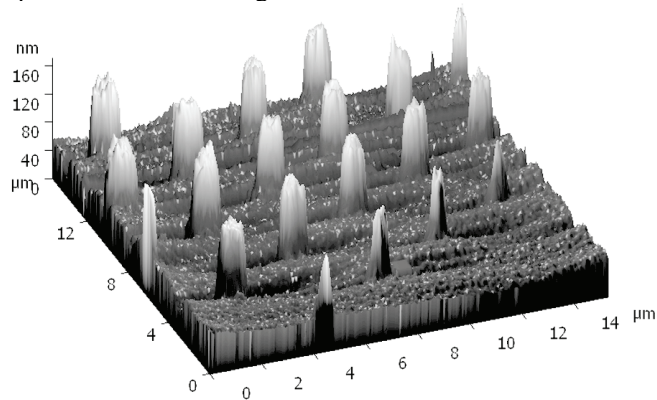


Fig. 4. AFM micrograph of an array of nanopillars near the edge of a single tooth in the serrate profile; the decreasing diameter is readily seen

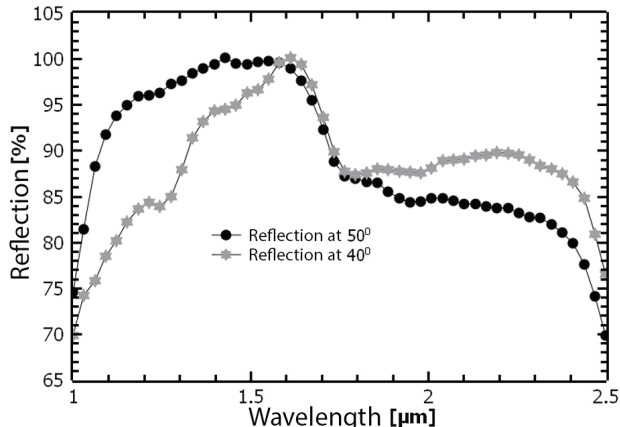


Fig. 5. Spectral dependence of reflected IR radiation for incident angles of 40° and 50°

It is readily observed that measured reflection is strongly dependent on the incident angle. This is due to the diffractive properties of the samples which behave as nonuniform diffractive gratings with angularly dependent diffraction efficiency. For the incident angles 40° and 50° the sample reflection is large and approaches 100% at some wavelengths, Fig. 5. At 60° reflection significantly drops, Fig. 6, reaching about 10%. An oscillatory character of the measurement reflectance spectra is noticeable at 60°, with a distance between subsequent peaks of about 70 nm.

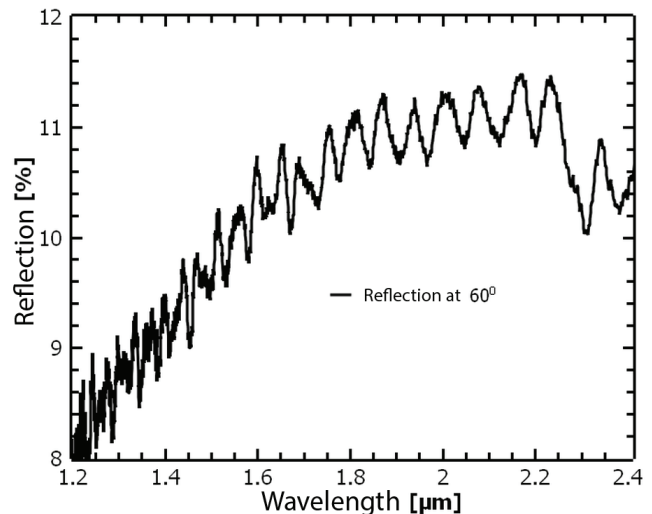


Fig. 6. Spectral dependence of reflected IR radiation for an incident angle of 60°

Samples were photographed in visible spectrum using an optical microscope, Fig. 7. The stripes with linearly varying pillar radii are readily seen. Each 100 μm stripe consists of 25 rows of pillars.



Fig. 7. Optical micrograph of graded pillar-based structure taken in white light. Several periods of the sawtooth-form array are visible

Figure 8 shows a photograph of 5 mm × 5 mm submicrometer pillar array on a microscopic glass substrate. White light illumination has been used. 100 μm wide stripes are readily observed. Reflected maxima corresponding to various diffracted orders are also seen. Parts of the background behind the glass substrate are visible in the locations of reflected minima.

V. CONCLUSION

A metal-dielectric structure with graded effective refractive index based on 2D submicrometer pillar array has been considered theoretically and experimentally. Superresolutions below the nominal resolution of the equipment have been obtained. The structures can be used as a basis for different metamaterial and plasmonic structures, including those for

transformation optics. In our future work we intend to utilize the fabricated geometry as a building block for sensing applications and to investigate the possibility of the use for transformation optics.

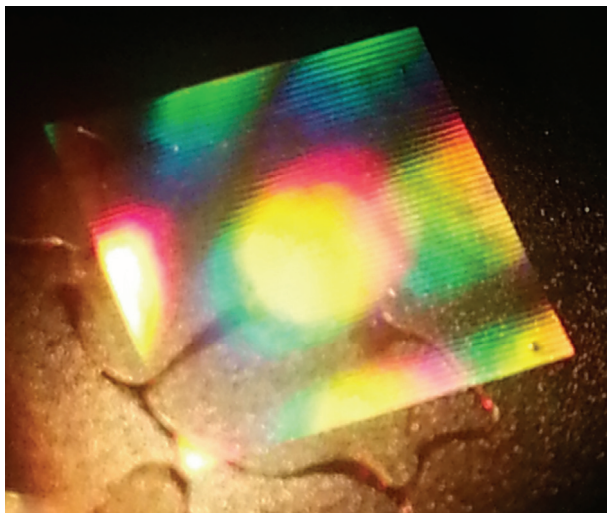


Fig. 8. White-light photograph of graded pillar-based structure. The base of the 2D array is 5 mm. Each stripe corresponds to a single period of the graded metamaterial ($a = 100 \mu\text{m}$)

ACKNOWLEDGEMENT

This is an extended version of the paper "Gradient-Index Infrared Metamaterials Based on Metal-Dielectric Submicrometer Pillar Arrays" presented at the 11th International Conference on Telecommunications in Modern Satellite, Cable and Broadcasting Services - TELSIKS 2013, held in October 2013 in Niš, Serbia. This work has been partially funded by Serbian Ministry of Education, Science and Technological Development within the framework of the project TR 32008.

REFERENCES

- [1] W. Cai, and V. Shalaev, *Optical Metamaterials: Fundamentals and Applications*, Springer, Dordrecht, Germany, 2009.
- [2] J.B. Pendry, D. Schurig, and D.R. Smith, "Controlling Electromagnetic Fields," *Science*, vol. 312, no. 5781, pp. 1780-1782, 2006.
- [3] P. W. Milloni, *Fast Light, Slow Light and Left-Handed Light*, Taylor & Francis, 2010.
- [4] Z. Jakšić, "Optical metamaterials as the platform for a novel generation of ultrasensitive chemical or biological sensors," *Metamaterials: Classes, Properties and Applications*, E. J. Tremblay, ed., pp. 1-42, Hauppauge, New York: Nova Science Publishers, 2010.
- [5] A. Lakhtakia, B. Michel, and W. S. Weiglhofer, "The role of anisotropy in the Maxwell Garnett and Bruggeman formalisms for uniaxial particulate composite media," *J. Phys. D*, vol. 30, no. 2, pp. 230-240, 1997.
- [6] D.R. Smith, J.J. Mock, A.F. Starr, and D. Schurig, "Gradient index metamaterials," *Phys. Rev. E*, vol. 71, no. 3, pp. 036609, 2005.

- [7] N. Dalarsson, M. Maksimović, and Z. Jakšić, "A simplified analytical approach to calculation of the electromagnetic behavior of left-handed metamaterials with a graded refractive index profile," *Sci. Sint.*, vol. 39, no. 2, pp. 185-191, 2007.
- [8] H.T. Chen, J.F. O'Hara, A.K. Azad, A.J. Taylor, R.D. Averitt, D. B. Shrekenhamer, and W. J. Padilla, "Experimental demonstration of frequency-agile terahertz metamaterials," *Nat. Photonics*, vol. 2, no. 5, pp. 295-298, 2008.
- [9] C. Gomez-Reino, M. Victoria Perez, C. Bao, *Gradient-Index Optics: Fundamentals and Applications*, Springer Verlag, Berlin-Heidelberg, 2002.
- [10] E. Merchand, *Gradient Index Optics*, Academic Press, New York, 1978.
- [11] D.T. Moore, "Gradient-index optics: a review," *Appl. Opt.*, vol. 19, no. 7, pp. 1035-1038, 1980.
- [12] J.B. Pendry, D. Schurig, and D.R. Smith, "Controlling Electromagnetic Fields," *Science*, vol. 312, no. 5781, pp. 1780-1782, 2006.
- [13] A.V. Kildishev, and V.M. Shalaev, "Engineering space for light via transformation optics," *Opt. Lett.*, vol. 33, no. 1, pp. 43-5, Jan 1, 2008.
- [14] H. Chen, C.T. Chan, and P. Sheng, "Transformation optics and metamaterials," *Nat. Mater.*, vol. 9, no. 5, pp. 387-396, 2010.
- [15] W. Cai, U.K. Chettiar, A.V. Kildishev, and V.M. Shalaev, "Optical cloaking with metamaterials," *Nat. Photonics*, vol. 1, no. 4, pp. 224-227, 2007.
- [16] J. Valentine, J. Li, T. Zentgraf, G. Bartal, and X. Zhang, "An optical cloak made of dielectrics," *Nat. Mater.*, vol. 8, no. 7, pp. 568-571, 2009.
- [17] H. Gao, B. Zhang, S. G. Johnson, and G. Barbastathis, "Design of thin-film photonic metamaterial Lüneburg lens using analytical approach," *Opt. Express*, vol. 20, no. 2, pp. 1617-1628, 2012/01/16, 2012.
- [18] V.N. Smolyaninova, I.I. Smolyaninov, A.V. Kildishev, and V. M. Shalaev, "Maxwell fish-eye and Eaton lenses emulated by microdroplets," *Opt. Lett.*, vol. 35, no. 20, pp. 3396-3398, 2010/10/15, 2010.
- [19] N.I. Landy, S. Sajuyigbe, J.J. Mock, D.R. Smith, and W.J. Padilla, "Perfect metamaterial absorber," *Phys. Rev. Lett.*, vol. 100, no. 20, 2008.
- [20] A.I. Fernández-Domínguez, S.A. Maier, and J.B. Pendry, "Collection and concentration of light by touching spheres: A transformation optics approach," *Phys. Rev. Lett.*, vol. 105, no. 26, 2010.
- [21] Z. Jacob, L.V. Alekseyev, and E. Narimanov, "Optical hyperlens: Far-field imaging beyond the diffraction limit," *Opt. Express*, vol. 14, no. 18, pp. 8247-8256, 2006.
- [22] Z. Liu, H. Lee, Y. Xiong, C. Sun, and X. Zhang, "Far-field optical hyperlens magnifying sub-diffraction-limited objects," *Science*, vol. 315, no. 5819, pp. 1686, 2007.
- [23] S.M. Vuković, Z. Jakšić, I. V. Shadrivov, and Y. S. Kivshar, "Plasmonic crystal waveguides" *Appl. Phys. A*, vol. 103, no. 3, pp. 615-617, 2011.
- [24] M. Dalarsson, M. Norgren, and Z. Jakšić, "Lossy gradient index metamaterial with sinusoidal periodicity of refractive index: Case of constant impedance throughout the structure," *J. Nanophotonics*, vol. 5, no. 1, pp. 051804, 2011.
- [25] M. Dalarsson, M. Norgren, N. Dončov, and Z. Jakšić, "Lossy gradient index transmission optics with arbitrary periodic permittivity and permeability and constant impedance throughout the structure," *Journal of Optics*, vol. 14, no. 6, pp. 065102, 2012.